Published in final edited form as:

J Cell Sci. 2007 November 15; 120(Pt 22): 3999–4008. doi:10.1242/jcs.009241.

Absence of keratin 19 in mice causes skeletal myopathy with mitochondrial and sarcolemmal reorganization

Michele R. Stone[1,*,‡],

Andrea O'Neill[1,*],

Richard M. Lovering[1,*],

John Strong[1],

Wendy G. Resneck[1],

Patrick W. Reed[1],

Diana M. Toivola[2,3],

Jeanine A. Ursitti[4],

M. Bishr Omary[2,3],

Robert J. Bloch[1,§]

[1]Department of Physiology, University of Maryland School of Medicine, Baltimore, MD 21201, USA

[2]Department of Medicine, Palo Alto VA Medical Center, 3801 Miranda Avenue, Mail code 154J, Palo Alto, CA 94304, USA

[3]Stanford University Digestive Disease Center, 300 Pasteur Drive, Stanford, CA 94305, USA

[4]Medical Biotechnology Center, University of Maryland Biotechnology Institute, Baltimore, MD 21201, USA

Summary

Intermediate filaments, composed of desmin and of keratins, play important roles in linking contractile elements to each other and to the sarcolemma in striated muscle. We examined the contractile properties and morphology of fast-twitch skeletal muscle from mice lacking keratin 19. Tibialis anterior muscles of keratin-19-null mice showed a small but significant decrease in mean fiber diameter and in the specific force of tetanic contraction, as well as increased plasma creatine kinase levels. Costameres at the sarcolemma of keratin-19-null muscle, visualized with antibodies against spectrin or dystrophin, were disrupted and the sarcolemma was separated from adjacent myofibrils by a large gap in which mitochondria accumulated. The costameric dystrophin-dystroglycan complex, which co-purified with γ-actin, keratin 8 and keratin 19 from striated muscles of wild-type mice, co-purified with γ-actin but not keratin 8 in the mutant. Our results suggest that keratin 19 in fast-twitch skeletal muscle helps organize costameres and links them to the contractile apparatus, and that the absence of keratin 19 disrupts these structures, resulting in loss of contractile force, altered distribution of mitochondria and mild myopathy. This

[§]Author for correspondence (rbloch@umaryland.edu).

[‡]Present address: Canon Life Sciences, Inc., Rockville, MD 20850, USA

[*]These authors contributed equally to this work

is the first demonstration of a mammalian phenotype associated with a genetic perturbation of keratin 19.

Keywords

Costamere; Sarcomere; Desmin; Dystrophin; Sarcolemma; Spectrin

Introduction

The sarcolemma of striated muscle, consisting of the plasma membrane and nearby cytoskeleton and extracellular matrix, is highly organized into regular structures that, in healthy muscle, are tightly linked to superficial elements of the contractile apparatus. These structures, termed ‘costameres’ (Pardo et al., 1983), have several functions, including the transmission of force and the stabilization of the membrane during the contractile cycle. Mutation of proteins that concentrate at costameres, and the subsequent disruption of their regular organization, occurs in several muscular dystrophies and myopathies (O’Neill et al., 2002; Porter et al., 1992; Reed et al., 2006; Reed et al., 2004; Williams and Bloch, 1999), suggesting that the maintenance of costameres is likely to be important for the long term health of striated muscle. Despite their evident importance, however, the functions of costameric proteins and their interactions at the plasma membrane are still poorly understood.

Costameres in rodent fast-twitch skeletal muscle consist of three distinct structures: Z-domains, which are linked to the Z-disks of nearby myofibrils; M-domains, which align with M-lines in nearby sarcomeres, and longitudinally oriented or L-domains, which lie parallel to the long axis of the myofibers and have no known correlate in the fiber interior (Bloch and Gonzalez-Serratos, 2003; Ervasti, 2003). Three types of cytoplasmic filaments link costameres to the underlying contractile apparatus.

γ-Actin, which comprises the best characterized of these filaments, associates with the sarcolemma – at least in part – through its ability to bind to dystrophin and, through dystrophin, to the dystrophin-associated glycoprotein complex (Ervasti and Campbell, 1993; Ibraghimov-Beskrovnaya et al., 1992; Rybakova et al., 2000). Dystrophin, the protein missing or mutated in Duchenne and Becker muscular dystrophies, has an N-terminal actin-binding domain that binds F-actin microfilaments with an affinity of ~10–50 μM (Renley et al., 1998; Rybakova et al., 1996; Senter et al., 1993; Sutherland-Smith et al., 2003) but its association with actin is enhanced by sequences in its rod domain (Amann et al., 1998; Warner et al., 2002; Rybakova and Ervasti, 2005). Dystrophin-actin interactions at the sarcolemma are important, because the absence of dystrophin in a murine muscular dystrophy weakens the association of γ-actin with the Z-domains of costameres (Rybakova et al., 2000), severely altering the organization of costameres (Williams and Bloch, 1999).

Two other structures, both composed of intermediate filaments (IFs), also link the contractile apparatus to the sarcolemma in striated muscle. One contains desmin, a type III IF protein; the other is composed of keratin 19 (K19) and keratin 8 (K8), which are, respectively, type I and type II IF proteins. Types I and II proteins must heterodimerize to assemble into

the larger, 10-nm diameter strands typical of IFs. Desmin forms homopolymers that are 10 nm in diameter, but it can also heteropolymerize with other type III intermediate filament proteins, which in adult muscle is most likely to be synemin (Bellin et al., 1999; Bellin et al., 2001; Hirako et al., 2003).

Desmin is the most abundant IF protein in mature striated muscle (reviewed in Capetanaki et al., 2007), where it surrounds each Z-disk and extends from the Z-disks of superficial myofibrils to the Z-domains of costameres at the sarcolemma. Desmin filaments are probably linked to costameres through plectin (Hijikata et al., 2003) and through the binding of synemin to dystrophin (Bhosle et al., 2006), the dystrophin-binding protein α-dystrobrevin (Mizuno et al., 2001; Mizuno et al., 2004), and other costameric components (Bellin et al., 2001). Mutations in desmin have been linked to myopathies (e.g. Dagvadorj et al., 2003; Dalakas et al., 2000; Munoz-Marmol et al., 1998; Schroder et al., 2003; Sjoberg et al., 1999), although the pathological basis of desminopathies is still unclear (Hoffman, 2003; Paulin et al., 2004). Elimination of desmin by homologous recombination disrupts costameres, especially at Z-domains (O'Neill et al., 2002), but it has otherwise surprisingly mild effects on striated muscle (Sam et al., 2000; Boriek et al., 2001; Haubold et al., 2003; Shah et al., 2004), which, however, include a redistribution of mitochondria in cardiac and slow-twitch fibers (Li et al., 1997; Milner et al., 2000).

K8 and K19 are also expressed in mature striated muscle (Ursitti et al., 2004). Although they are harder to detect and are present in smaller amounts than desmin, K8 and K19 are found at both the Z-disks and M-lines of myofibrils near the sarcolemma (Ursitti et al., 2004), where they are appropriately localized to link myofibrils to the M- and Z-domains of costameres. Deeper in the myofibers, they, like desmin, concentrate primarily around Z-disks (Ursitti et al., 2004). At the sarcolemma, they are also enriched at the L-domains and are thus the most likely cytoplasmic structures to stabilize the L- and M-domains of costameres. When overexpressed in skeletal myofibers, K8 accumulates in the middle of sarcomeres (Stone et al., 2005), suggesting an affinity for the proteins of M-bands. Both K8 and K19 co-purify with the dystrophin-dystroglycan complex (Ursitti et al., 2004). Consistent with this, keratin filaments containing K19 specifically interact with a fragment of dystrophin in COS-7 cells and in vitro, and overexpression of K19 in adult myofibers disrupts the association of dystrophin with costameres (Stone et al., 2005).

Here, we examine the structure and function of skeletal muscle lacking K19. $K19^{-/-}$ mice were developed by Tamai et al. (Tamai et al., 2000) to examine the role of this protein in the tissues in which it was then known to be expressed, especially in developing embryos and in epithelial cells of the gut and kidney. Remarkably, the absence of K19 showed no phenotype in these tissues, probably owing to the presence of other type I keratins, because crossing with K8- or K18-null mice is embryonic lethal (Tamai et al., 2000; Hesse et al., 2000). This left the possible role of K19 in epithelial cells and other tissues in which it is expressed unresolved. We decided to address this question in muscle, pursuant to our discovery of K19 in mature cardiac and skeletal muscle (Ursitti et al., 2004). We report here that fast-twitch skeletal muscle from $K19^{-/-}$ mice has a mild myopathy. Our experiments are therefore the first to show a phenotype associated with the absence of K19 in mammalian tissues.

Results

We studied fast-twitch muscles from K19$^{-/-}$ mice, to learn how this type I IF protein contributed to muscle structure and function. Genotypes of the mice we used were confirmed by PCR of tail snips (not shown). Assays using reverse transcriptase coupled with PCR (RT-PCR) confirmed the presence of mRNA encoding K19 in wild-type but not in K19$^{-/-}$ muscle (Fig. 1A). mRNA encoding K8, which heterodimerizes with K19, is present in both control and K19$^{-/-}$ samples (Fig. 1A). Immunoprecipitation followed by immunoblotting confirmed the absence of K19 in K19$^{-/-}$ tibialis anterior (TA) muscle (Fig. 1B). Immunoblots of K8 and desmin in extracts of K19$^{-/-}$ TA muscle showed levels of K8 that were not significantly altered from wild type (Fig. 1C), but did show a small but significant increase in desmin (Fig. 1C; 24±3% elevation compared with controls, n=3, P<0.01, t-test). This increase was not seen in gastrocnemius muscle, however (not shown).

The physiological properties of fast-twitch muscle were affected by the absence of K19. In particular, TA muscles from K19$^{-/-}$ mice generated less force during maximal tetanic contractions, compared with controls (Table 1). Their mass was also reduced, but this reduction was not sufficient to account for the decrease in contractile force during tetanic stimulation, because specific force (force normalized to cross-sectional area of the muscle) was diminished by ~15% in TA muscles lacking K19 (Fig. 2, black bars; P<0.05, t-test). This change could not be explained by changes in fiber type, because the relative number of slow fibers in TA muscles of K19$^{-/-}$ mice, identified with antibodies to slow myosin (Fig. 3C,D) increased, only marginally, to ~10% of the total fibers in the mutant (Table 1; P<0.05, t-test). Assuming a difference in specific tension between fast and slow fibers of ~30% (Bodine et al., 1987), the shift in fiber type should account for only an ~3% decrease in specific force. As we measured a ~15% decrease (Fig. 2), the increase in slow fibers is not large enough to account for the decrease in specific force observed in K19$^{-/-}$ muscle. Injury caused by a single, high-strain lengthening (eccentric) contraction was also greater in K19$^{-/-}$ TA muscle (24±8%, mean ± s.d.) than in controls (16.5±6%; Fig. 2, gray bars), but this difference was not significant for the number of animals we have analyzed (n=6 per group; P>0.1, paired t-test). The lower mass and decreased specific force indicate that the absence of K19 is linked to a mild myopathy.

Morphological and biochemical tests supported this conclusion. The average diameter of myofibers in the TA muscles of K19$^{-/-}$ mice were smaller, and the range of myofiber diameters were larger, than in wild type (Fig. 3). Upon quantitation, the mean minimal Feret's diameter was significantly smaller in K19$^{-/-}$ TA muscles compared to controls (P<0.001; Mann-Whitney rank sum test; Table 1). Plasma levels of creatine kinase were also elevated, to a level ~threefold greater than control values (Table 1). Although this was ~tenfold less than the levels of dystrophic *mdx* mice (not shown), it was nevertheless significantly higher than wild type (P<0.001, t-test) and consistent with levels seen in some patients with myopathy (Flanigan, 2004). Neither the permeability of TA myofibers to Evans Blue dye nor the number of fibers with central nuclei were significantly different from age-matched controls (P>0.05, ξ^2 test; Table 1; see also Fig. 3A,B), nor were centrally nucleated fibers elevated in diaphragm muscle of K19$^{-/-}$ mice (not shown). Similarly, neither wild-type nor K19$^{-/-}$ TA muscles showed significant levels of apoptosis, assayed

by TUNEL staining, or significant differences in their myogenic capacity, assayed after injection of cardiotoxin (data not shown). These results are consistent with a mild skeletal myopathy in the $K19^{-/-}$ mouse that does not involve a high level of muscle degeneration and regeneration.

We studied TA muscles by electron microscopy to learn whether the absence of K19 significantly altered the contractile apparatus. Our results (Fig. 4A–C) showed that the organization of sarcomeres and the lateral alignment of myofibrils are not greatly altered in $K19^{-/-}$ mice. There was, however, a small but significant increase in the distances between Z-disks of neighboring myofibrils, from 0.18±0.01μm (mean ± s.e.m., n=79) to 0.24±0.01 μm (mean ± s.e.m., n=75; P<0.0001, two-tailed t-test: Fig. 4D), consistent with a role for K19 in forming the lateral links between myofibrils.

Our ultrastructural studies revealed a notable change in the distribution of mitochondria and the relationship of the sarcolemma to the underlying contractile apparatus (Fig. 4A–C,E,F). In controls, the sarcolemma was closely apposed to superficial myofibrils, with an average gap of 0.15±0.02 μm (mean ± s.e.m., n=68). In $K19^{-/-}$ TA muscle, the average gap between the sarcolemma and the nearest myofibrils was 0.99±0.10 μm (mean ± s.e.m., n=74). Values for individual measurements are shown in Fig. 4F. This difference was highly significant (P<0.0001, two-tailed t-test).

Equally striking was the presence of large numbers of mitochondria in the subsarcolemmal gap in $K19^{-/-}$ TA muscle (Fig. 4B,C,E). Mitochondria are only rarely present between the myofibrils and the sarcolemma in controls (Fig. 4A), consistent with published reports (e.g. Gauthier, 1979). This change in morphology was quantified from electron microscopic images and found to be significant (P<0.001, ξ^2, test n=302 fibers for wild type, 346 for $K19^{-/-}$; Fig. 4E). Ultrastructural studies of the extensor digitorum longus muscle indicate that mitochondria also accumulate under the sarcolemma of this fast-twitch muscle when K19 is absent (not shown). By contrast, electron micrographs of $K19^{-/-}$ soleus muscle, which has ~60% slow-twitch fibers, showed no significant differences in the organization of mitochondria (P>0.6, ξ^2 test, n=347 fibers for wild type, 344 for $K19^{-/-}$; Fig. 4E). Indeed, most soleus myofibers in controls showed accumulations of mitochondria near the sarcolemma, as reported (Gauthier, 1979), making possible differences with $K19^{-/-}$ muscle difficult to discern. These results suggest that K19 contributes significantly to the subcellular localization of mitochondria in fast-twitch but not in slow-twitch muscles. This specificity with respect to muscle fiber type is consistent with a previous report that subsarcolemmal mitochondria increase in cardiac and slow-twitch, but not fast-twitch, muscles of desmin-null mice (Milner et al., 2000).

The altered relationship between the sarcolemma and the contractile apparatus should result in weakened links between costameres at the sarcolemma and the Z-disks and M-lines of superficial myofibrils. We examined longitudinal cryosections of TA muscle from control and $K19^{-/-}$ mice to test this possibility. We found that the costameric proteins, βI-spectrin and dystrophin, as well as vinculin (not shown), redistributed at the sarcolemma of ~30% of the myofibers (Fig. 5D–I, Fig. 6). By contrast, desmin (Fig. 5G–I) and α-actinin (not shown), both of which associate with Z-disks, were not notably altered in myofibrils

visualized in the same sections, consistent with our ultrastructural results. The quantitative differences in the organization of β-spectrin at the sarcolemma in TA muscles from control and K19$^{-/-}$ mice (Fig. 6) were significant (P<0.01, Chi^2 test). Although not quantitated, changes in the sarcolemmal organization of dystrophin coincided with those observed for β-spectrin. We conclude that the contractile elements near the sarcolemma of TA muscles are relatively unaffected by the absence of K19, but that the organization of costameres at the sarcolemma is compromised.

The organization of dystrophin at costameres in wild-type muscle and its rearrangement in K19$^{-/-}$ muscle is consistent with the fact that the dystrophin-dystroglycan complex normally associates with K19 (Ursitti et al., 2004). We used affinity chromatography on a wheat germ lectin column to isolate the dystrophin-dystroglycan complex from wild-type and K19$^{-/-}$ muscle and then analyzed the enriched preparations. K8, K19 and γ-actin eluted together with dystrophin and β-dystroglycan from wild-type muscle, as reported (Ursitti et al., 2004), but only γ-actin and not K8 eluted with the complex from K19$^{-/-}$ tissue (Fig. 7). All binding to the column was specific, as it was inhibited by the inclusion of the sugar hapten, N-acetyl-glucosamine (not shown). These results show that the dystrophin-dystroglycan complex is retained in K19$^{-/-}$ muscle, where it associates with γ-actin but not K8.

Discussion

Intermediate filaments composed of K8 and K19 associate with costameres at the sarcolemma as well as with the contractile apparatus of striated muscle (Ursitti et al., 2004). Although both desmin-based IFs and actin microfilaments help link the Z-disks of superficial myofibrils to the sarcolemma, filaments containing K8 and K19 associate with all three costameric domains and are the only cytoplasmic structures known that are appropriately localized to stabilize the M- and L-domains. Consistent with this, keratins remain at costameres of some myofibers in the desmin-null mouse, suggesting that they may be capable of stabilizing these structures when desmin is missing (O'Neill et al., 2002). These observations led us to predict that the absence of keratin subunits would destabilize costameres. As costameres provide a lateral pathway for force transmission in striated muscle (Bloch and Gonzalez-Serratos, 2003), we further predicted that elimination of keratins would reduce the specific force of contraction. Our studies of the K19$^{-/-}$ TA muscle of the mouse confirm these predictions and support the idea that keratin filaments, comprised in part of K19, help to organize costameres and to transmit contractile force. The absence of K19 does not cause the complete loss of costameres, however, perhaps because desmin and γ-actin and their association with costameric structures are not significantly altered. Alternatively, upregulation of other proteins, including other keratins, may mitigate the effects of the K19$^{-/-}$ phenotype. The changes that occur at costameres and nearby myoplasm of fast-twitch muscles of the K19$^{-/-}$ mouse are shown in schematic form in Fig. 8. This is the first example of a phenotype linked solely to the absence of K19.

Remarkably, in most myofibers lacking K19 the enlarged gap between the sarcolemma and the contractile apparatus of muscle is filled with mitochondria. The mild myopathy seen in K19$^{-/-}$ mice may be linked to this change in mitochondrial location, because subsarcolemmal mitochondria are not as metabolically efficient as intermyofibrillar

mitochondria (Adhihetty et al., 2007; Cogswell et al., 1993; Philippi and Sillau, 1994) The absence of K19 may release mitochondria from tethers deeper in the myoplasm, allowing them to accumulate in gaps that would otherwise remain large and filled with cortical cytoplasm, or it may mediate their active redistribution to beneath the sarcolemma, enlarging the gaps. Whatever the mechanism, the redistribution of mitochondria may be a common trait of striated muscle lacking functional IF proteins, as a similar result has been reported in slow-twitch muscle fibers and cardiac myocytes of the desmin-null mouse (Li et al., 1997; Milner et al., 2000), as well as in some human desminopathies (Schroder et al., 2003). We have not seen accumulation of mitochondria under the sarcolemma of fast-twitch myofibers in muscle lacking desmin, or of cardiomyocytes in the $K19^{-/-}$ mouse (our unpublished results), nor have we detected K19-dependent changes in mitochondrial distribution in slow-twitch soleus muscle (Fig. 4E). This suggests that different types of IFs control mitochondrial distribution in the various striated muscles: desmin-based filaments in cardiomyocytes and slow-twitch myofibers, and keratin-based filaments in fast-twitch muscle.

Mutations in intermediate filaments and plectin, which can associate with both intermediate filaments and mitochondria (Reipert et al., 1999), have been linked to mitochondrial defects in several murine and human diseases of muscle (Milner et al., 2000; Schroder et al., 2002; Schroder et al., 2003). Mutations in other types of IFs are also associated with changes in mitochondrial location or function in a variety of cell types (Toivola et al., 2005). Given the relatively mild myopathy in young $K19^{-/-}$ mice, the defects in mitochondrial function associated with mislocalization to regions under the sarcolemma of fast-twitch muscle fibers are likely to be modest. Nevertheless, some features of the myopathy seen in $K19^{-/-}$ muscles may be a consequence of mitochondrial redistribution, as suggested for cardiomyopathies in mice lacking desmin (Milner et al., 2000). We expect that the mitochondrial defects as well as the severity of the myopathy in mice lacking K19 will increase with age, as has also been reported for the desmin-null mouse (Li et al., 1997; Milner et al., 2000).

Although the cause is still unclear, our results clearly show that young $K19^{-/-}$ mice have a mild skeletal myopathy. In addition to the changes at the sarcolemma and its relationship to the contractile apparatus, and in the localization of mitochondria, fast-twitch muscle in the $K19^{-/-}$ mouse generates significantly less contractile force than wild-type controls. Plasma levels of creatine kinase are also elevated. As we have not yet observed significant changes in the morphologies of cardiac or slow-twitch skeletal muscle in these mice, the primary myopathy, and thus the source of creatine kinase in the plasma, is likely to be fast-twitch muscle that is compromised by the absence of K19. At least one muscular dystrophy, facioscapulohumeral muscular dystrophy (FSHD), is accompanied by relatively mild increases in plasma creatine kinase (Flanigan, 2004) and by increases in the gap between the sarcolemma and the contractile apparatus, with mild but marked alterations in the organization of costameres (Reed et al., 2006). As FSHD maps to chromosome 4q35tel in humans, whereas K19 maps to 17q21, FSHD is unlikely to be linked to defects in K19. Nevertheless, it is intriguing that some aspects of the phenotype are similar to those seen in a human muscular dystrophy.

In summary, we report that the absence of K19 in fast-twitch skeletal muscle is accompanied by a mild myopathy associated with disruption of costameres and altered distribution of mitochondria. Ours is the first report of a phenotype linked solely to the absence of K19. The fact that it appears in fast-twitch muscle, which until recently was not thought to express keratins at all (Ursitti et al., 2004), suggests that further study of muscles of $K19^{-/-}$ mice may provide new insights into the role of keratins in muscle function and disease.

Materials and Methods

Animals

FVB male and female mice homozygous for the K19 mutation were the kind gift of M.M. Taketo (Graduate School of Medicine, Kyoto University, Kyoto Japan). As reported (Tamai et al., 2000), these mice lack nearly the entire first exon of the K19 gene and fail to express either K19 mRNA or protein. They were bred and genotyped from tail snips as described (Hesse et al., 2000; Tamai et al., 2000), with the DNeasy (Qiagen, Valencia, CA) or Nucleon Genomic DNA (Tepnel Life Sciences, Manchester, UK) kits. The PCR reaction used either Taq Pro Red Complete DNA Polymerase (Denville Scientific, Metuchen, NJ) or the Accuprime PFX kit (Invitrogen Corp., Carlsbad, California).

Mice for functional and morphological studies were 1–3 months old and were anesthetized with ketamine and xylazine (40 mg/kg and 10 mg/kg body mass, respectively) before physiological testing and euthanasia, which was performed by perfusion fixation with 2% paraformaldehyde in buffered saline. As we found no significant differences between males and females, we combined our results for both sexes. Activity of creatine kinase in plasma was assayed as described (Teixeira et al., 2003). The Institutional Animal Care Committee of the University of Maryland School of Medicine approved all our protocols.

RT-PCR

mRNA was prepared with TRIzol (Invitrogen) and used with the Super Script First Strand Synthesis system (Invitrogen), as recommended by the supplier. PCR was used to probe the reverse-transcribed mRNAs for K19 and K8 sequences (GenBank accession number M21836.1), with the primers: (forward) 5′-CTACCTTGCTCGGATTGAGGAG-3′ (K19) and 5′-ACATGAGCATTATACGAAGACC-3′ (K8); (reverse) 5′-AGTCTCGCTGGTAGCTCAGATG-3′ (K19) and 5′-CACTCTGCCATACAGCTGTCT-3′ (K8).

Immunofluorescence labeling

Tibialis anterior (TA) muscles were perfusion-fixed, dissected, snap frozen, and labeled by immunofluorescence (O'Neill et al., 2002). We used chicken antibodies against βI-spectrin (Ursitti et al., 2001) to label costameres (e.g. O'Neill et al., 2002). Rabbit antibodies were to dystrophin and desmin (used at 1:100; Lab Vision, Fremont, CA); mouse antibodies were to the fast-twitch or slow-twitch isoform of the myosin heavy chain (1:500; Sigma, St Louis, MO). Myofibers were also labeled with anti-βI-spectrin and 5 μg/ml propidium iodide (Sigma/Aldrich) to label nuclei. Samples were mounted and examined under confocal optics (O'Neill et al., 2002; Reed et al., 2004), and scored for the predominant pattern of

organization of βI-spectrin at the sarcolemma. Patterns were categorized as normal (i.e. costameres with Z-, M- and L-domains; score=3), partially organized (costameres with only one remaining set of domains, typically Z-domains; score=2), or extensively disorganized (absence of costameres over large sarcolemmal areas; score=1) (Reed et al., 2004).

Some mice were injected intraperitoneally with 10 mg/ml Evans Blue dye (Sigma) in buffered saline (Lovering and De Deyne, 2004) before muscles were fixed and processed, as above. Myofibers with dye-labeled sarcoplasm were quantified in cross-sections under fluorescence optics (Lovering and De Deyne, 2004). At least 400 fibers in ten optical fields were assessed in three mice, and results are expressed as percent labeled fibers.

Ultrastructure and morphometry

Perfusion-fixed TA muscles were removed and incubated overnight in 2% glutaraldehyde, 2 mg/ml tannic acid, 0.2 M cacodylate, pH 7.2, then stained with heavy metals, dehydrated, post-fixed in 1% osmium tetroxide in 0.5 M acetate buffer, en bloc stained with 1% uranyl acetate, dehydrated, embedded in Araldite-Embed 812 resin, sectioned for electron microscopy at 90 nm, and viewed with a Phillips 201 microscope. Images were taken on Kodak 4489 film and digitally scanned at 600 dpi. Distances between the sarcolemma and the nearest myofibrils, and between neighboring myofibrils in the interior of the myofiber, were measured from negative images of longitudinal sections of all myofibers examined, using Scion Image (Scion Corp., Frederick, MD). Mitochondrial accumulations under the sarcolemma were scored as slight (<10% of the sarcolemma underlain by mitochondria), moderate (10–50% of the sarcolemma underlain by mitochondria) or large (>50% underlain by mitochondria) from cross sections viewed under the electron beam at a magnification of × 15,000.

The relative sizes of myofibers were determined from frozen cross sections labeled with anti-βI-spectrin. Images were obtained under confocal optics, imported into CorelDraw (Corel Corp., Ltd, Ottawa, Canada), and the minimal Feret's diameter was measured for at least 100 muscle fibers from each mouse with a digital caliper (Briguet et al., 2004). TUNEL staining (Apoptag, Chemicon, Temecula, CA) was used to label apoptotic nuclei (Gavrieli et al., 1992).

Muscle force measurements

Contractile function of isolated TA muscle was studied as described for rats (Lovering et al., 2007; Lovering and De Deyne, 2004), with slight changes in the stimulation protocol (Barash et al., 2004). We used six WT and six $K19^{-/-}$ mice to compare contractile function before and after injury. We attached the TA to a load cell and applied single twitches (rectangular pulse, 1 msecond) at different muscle lengths to determine the optimal length (resting length L_0, measured with calipers as the distance between the tibial tuberosity and the myotendinous junction). With muscles set at L_0, we gradually increased the stimulation frequency to establish a force-frequency relationship. We obtained a maximally fused, tetanic contraction at 200 Hz (300-msecond train duration of 1-msecond pulses at a constant current of 5 mA). We used 150% of the maximal stimulation intensity to induce maximal activation of contraction (tension, P_0). Maximal tetanic tension was measured after

5 minutes of continuous stimulation at 1 Hz and expressed as a percentage of P_0, to provide an index of fatigue. The cross-sectional area for each muscle was determined by dividing the mass of the muscle by the product of its optimum fiber length (L_f) and fiber density (DelloRusso et al., 2001). L_f was determined by multiplying L_0 of the TA by 0.6, the ratio of L_f/L_0 (Burkholder et al., 1994). Density of mammalian skeletal muscle is 1.06 g/cm^3 (Mendez and Keys, 1960). Muscle output was then expressed as specific force (kN/m^2), determined by dividing the tension by the muscle cross-sectional area.

Muscle injury

Injury induced by a single maximal lengthening contraction was performed in mice, as previously described for rats (Lovering et al., 2005; Lovering et al., 2007; Lovering and De Deyne, 2004), with minor modifications. Briefly, mice were anesthetized with intraperitoneal ketamine and xylazine (40 mg/kg and 10 mg/kg body mass, respectively). With the animal supine, the hindlimb was stabilized and the foot was secured onto a plate, the axis of which was attached to a stepper motor (model T8904, NMB Technologies, Chatsworth, CA) and a potentiometer to measure range of motion of the ankle. A custom program (Labview version 4.1, National Instruments, Austin, TX) was used to synchronize contractile activation and the onset of ankle rotation. The foot was stabilized to the footplate and moved into plantarflexion through a 90° arc of motion (−10° to 80°, with the foot orthogonal to the tibia considered as 0°) at an angular velocity of 900° per second, initiated 200 mseconds after tetanic stimulation of the TA.

Regeneration after cardiotoxin injection

To compare regeneration between WT and K19$^{-/-}$ mice, we injected cardiotoxin (Sigma; 0.1 ml 10 μm in PBS) into the TA muscle to induce necrotic cell death followed by myogenesis (Yan et al., 2003). The TA muscles of three WT and three K19$^{-/-}$ mice were harvested at days 7 and 14 after injection, snap frozen, and stained with hematoxylin and eosin. The number of centrally nucleated fibers (CNFs) were counted in a blind fashion and quantified as a percentage of all of the fibers analyzed.

Protein separation and analysis

For immunoprecipitation, TA muscles from adult mice were harvested and frozen in liquid nitrogen. Frozen muscle samples (1 mg) were homogenized with a PowerGen 125 homogenizer (Fisher Scientific, Waltham MA) at a w/v ratio of 0.05 in homogenate buffer (10 mM NaPO4, 2 mM EDTA, 140 mM NaCl, 1% NP40, pH 7.4) with protease inhibitors (Complete Protease Inhibitor Tablets, Roche Diagnostics). The homogenates were incubated on ice for 1 h. Immunoprecipitations were performed from this homogenate with goat anti-mouse M450 Dynabeads® (Dynal, Lake Success, NY), according to the manufacturer's instructions, and monoclonal antibodies against keratin 19 (Progen Biotechnik, Germany), or a non-immune, control antibody (MOPC-141, Sigma). After separation on a 4–12% NuPAGE polyacrylamide-gradient gel (Invitrogen, Carlsbad, CA), proteins in the immunoprecipitates were immunoblotted as described (Ursitti et al., 2004). Purified recombinant human keratin 19 (Research Diagnostics, Inc., Flanders, NJ) was used as a positive control. Equal loading and transfer was confirmed by Ponceau S staining.

The dystrophin-dystroglycan complex was purified from homogenates of hearts from young adult mice by affinity chromatography on a wheat germ lectin column (Ervasti et al., 1991; Ursitti et al., 2004). Non-specific binding was assessed by the inclusion of 0.3 M N-acetylglucosamine in the loading buffer, which prevented binding of glycoproteins to the lectin matrix. Proteins bound to the lectin column were eluted by boiling in sample buffer, separated by SDS-PAGE, transferred electrophoretically to nitrocellulose and immunoblotted for dystrophin (dys-2, Novacastra, Newcastle-upon-Tyne, UK), β-dystroglycan (Novacastra), γ-actin (gift of J. Chloe Bulinski, Columbia University, New York, NY), K8 (Troma I, Developmental Studies Hybridoma Bank, University of Iowa, Iowa City, IA) and K19. Secondary antibodies conjugated to alkaline phosphatase were from Jackson Immunoresearch (West Chester, PA). Labeled bands were visualized chromogenically (Western Light, Tropix Laboratories, Bedford, MA).

Acknowledgments

We thank D. W. Pumplin for assistance with morphometry and statistics. Our work is supported by a Muscular Dystrophy Association grant no. 3371 (R.J.B.), and NIH grant DK47918 and VA Merit Support (M.B.O.). M.R.S. was supported by training grant T32 HL 080711 (T. Pallone) and R.M.L. by an N.R.S.A. (1F32 HD 047099) and by a Development Award from the Muscular Dystrophy Association (no. 4278). P.R. is the recipient of a Bronfman Award from the FSH Society.

References

Adhihetty PJ, O'Leary MF, Chabi B, Wicks KL and Hood DA (2007). Effect of denervation on mitochondrially mediated apoptosis in skeletal muscle. J. Appl. Physiol 102, 1143–1151. [PubMed: 17122379]

Amann KJ, Renley BA and Ervasti JM (1998). A cluster of basic repeats in the dystrophin rod domain binds F-actin through an electrostatic interaction. J. Biol. Chem 273, 28419–28423. [PubMed: 9774469]

Barash IA, Mathew L, Ryan AF, Chen J and Lieber RL (2004). Rapid muscle-specific gene expression changes after a single bout of eccentric contractions in the mouse. Am. J. Physiol. Cell Physiol 286, C355–C364. [PubMed: 14561590]

Bellin RM, Sernett SW, Becker B, Ip W, Huiatt TW and Robson RM (1999). Molecular characteristics and interactions of the intermediate filament protein synemin. Interactions with alpha-actinin may anchor synemin-containing heterofilaments. J. Biol. Chem 274, 29493–29499. [PubMed: 10506213]

Bellin RM, Huiatt TW, Critchley DR and Robson RM (2001). Synemin may function to directly link muscle cell intermediate filaments to both myofibrillar Z-lines and costameres. J. Biol. Chem 276, 32330–32337. [PubMed: 11418616]

Bhosle RC, Michele DM, Campbell KP, Li Z and Robson RM (2006). Interactions of intermediate filament protein synemin with dystrophin and utrophin. Biochem. Biophys. Res. Commun 346, 768–777. [PubMed: 16777071]

Bloch RJ and Gonzalez-Serratos H (2003). Lateral force transmission across costameres in skeletal muscle. Exerc. Sport Sci. Rev 31, 73–78. [PubMed: 12715970]

Bodine SC, Roy RR, Eldred E and Edgerton VR (1987). Maximal force as a function of anatomical features of motor units in the cat tibialis anterior. J. Neurophysiol 57, 1730–1745 [PubMed: 3598628]

Boriek AM, Capetanaki Y, Hwang W, Officer T, Badshah M, Rodarte J and Tidball JG (2001). Desmin integrates the three-dimensional mechanical properties of muscles. Am. J. Physiol. Cell Physiol 280, C46–C52. [PubMed: 11121375]

Briguet A, Courdier-Fruh I, Foster M, Meier T and Magyar JP (2004). Histological parameters for the quantitative assessment of muscular dystrophy in the mdx mouse. Neuromuscul. Disord 14, 675–682. [PubMed: 15351425]

Burkholder TJ, Fingado B, Baron S and Lieber RL (1994). Relationship between muscle fiber types and sizes and muscle architectural properties in the mouse hindlimb. J. Morphol 221, 177–190. [PubMed: 7932768]

Capetanaki Y, Bloch RJ, Kouloumenta A, Mavroidis M, and Psarras S (2007). Muscle intermediate filaments and their links to membranes and membranous organelles. Exp. Cell Res 313, 2063–2076. [PubMed: 17509566]

Cogswell AM, Stevens RJ and Hood DA (1993). Properties of skeletal muscle mitochondria isolated from subsarcolemmal and intermyofibrillar regions. Am. J. Physiol. Cell Physiol 264, C383–C389.

Dagvadorj A, Goudeau B, Hilton-Jones D, Blancato JK, Shatunov A, Simon-Casteras M, Squier W, Nagle JW, Goldfarb LG and Vicart P (2003). Respiratory insufficiency in desminopathy patients caused by introduction of proline residues in desmin c-terminal alpha-helical segment. Muscle Nerve 27, 669–675. [PubMed: 12766977]

Dalakas MC, Park KY, Semino-Mora C, Lee HS, Sivakumar K and Goldfarb LG (2000). Desmin myopathy, a skeletal myopathy with cardiomyopathy caused by mutations in the desmin gene. N. Eng. J. Med 342, 770–780.

DelloRusso C, Crawford RW, Chamberlain JS and Brooks SV (2001). Tibialis anterior muscles in *mdx* mice are highly susceptible to contraction-induced injury. J. Muscle Res. Cell Motil 22, 467–475. [PubMed: 11964072]

Ervasti JM (2003). Costameres: the Achilles' heel of Herculean muscle. J. Biol. Chem 278, 13591–13594. [PubMed: 12556452]

Ervasti JM and Campbell KP (1993). A role for the dystrophin-glycoprotein complex as a transmembrane linker between laminin and actin. J. Cell Biol 122, 809–823. [PubMed: 8349731]

Ervasti JM, Kahl SD and Campbell KP (1991). Purification of dystrophin from skeletal muscle. J. Biol. Chem 266, 9161–9165. [PubMed: 2026615]

Flanigan KM (2004). Facioscapulohumeral muscular dystrophy and scapuloperoneal disorders. In Myology (3rd edn) (ed. Engel AG and Franzini-Armstrong C), pp. 1123–1134. New York: McGraw-Hill.

Gauthier GF (1979). Ultrastructural identification of muscle fiber types by immunocytochemistry. J. Cell Biol 82, 391–400. [PubMed: 383727]

Gavrieli Y, Sherman Y and Ben-Sasson SA (1992). Identification of programmed cell death in situ via specific labeling of nuclear DNA fragmentation. J. Cell Biol 119, 493–501. [PubMed: 1400587]

Hesse M, Franz T, Tamai Y, Taketo MM and Magin TM (2000). Targeted deletion of keratins 18 and 19 leads to trophoglast fragility and early embryonic lethality. EMBO J. 19, 5060–5070. [PubMed: 11013209]

Hijikata T, Murakami T, Ishikawa H and Yorifuji H (2003). Plectin tethers desmin intermediate filaments onto subsarcolemmal dense plaques containing dystrophin and vinculin. Histochem. Cell Biol 119, 109–123. [PubMed: 12610730]

Hirako Y, Yamakawa H, Tsujimura Y, Nishizawa Y, Okumura M, Usukura J, Matsumoto H, Jackson KW, Owaribe K and Ohara O (2003). Characterization of mammalian synemin, an intermediate filament protein present in all four classes of muscle cells and some neuroglial cells: co-localization and interaction with type III intermediate filament proteins and keratins. Cell Tissue Res. 313, 195–207. [PubMed: 12845519]

Hoffman EP (2003). Desminopathies: good stuff lost, garbage gained, or the trashman misdirected? Muscle Nerve 27, 643–645. [PubMed: 12766974]

Ibraghimov-Beskrovnaya O, Ervasti JM, Leveille CJ, Slaughter CA, Sernett SW and Campbell KP (1992). Primary structure of dystrophin-associated glycoproteins linking dystrophin to the extracellular matrix. Nature 355, 696–702 [PubMed: 1741056]

Li Z, Mericskay M, Agbulut O, Butler-Browne GS, Carlsson L, Thornell L-E, Babinet C and Paulin D (1997). Desmin is essential for the tensile strength and integrity of myofibrils but not for myogenic commitment, differentiation, and fusion of skeletal muscle. J. Cell Biol 139, 129–144. [PubMed: 9314534]

Lovering RM and De Deyne PG (2004). Contractile function, sarcolemma integrity and the loss of dystrophin after skeletal muscle eccentric contraction-induced injury. Am. J. Physiol. Cell Physiol 286, C230–C238. [PubMed: 14522817]

Lovering RM, Hakim M, Moorman CT III and De Deyne PG (2005). The contribution of contractile pre-activation to loss of function after a single lengthening contraction. J. Biomech 38, 1501–1507. [PubMed: 15922761]

Lovering RM, Roche JA, Bloch RJ and De Deyne PG (2007). Recovery of function in skeletal muscle following two different contraction-induced injuries. Arch. Phys. Med. Rehabil 88, 617–625. [PubMed: 17466731]

Mendez J and Keys A (1960). Density and composition of mammalian muscle. Metabolism 9, 184–188.

Milner DJ, Mavroidis M, Weisleder N and Capetanaki Y (2000). Desmin cytoskeleton linked to muscle mitochondrial distribution and respiratory function. J. Cell Biol 150, 1283–1297. [PubMed: 10995435]

Mizuno Y, Thompson TG, Guyon JR, Lidov HG, Brosius M, Imamura M, Ozawa E, Watkins SC and Kunkel LM (2001). Desmuslin, an intermediate filament protein that interacts with α-dystrobrevin and desmin. Proc. Natl. Acad. Sci. USA 98, 6156–6161. [PubMed: 11353857]

Mizuno Y, Guyon JR, Watkins SC, Mizushima K, Sasaoka T, Imamura M, Kunkel LM and Okamoto K (2004). Beta-synemin localizes to regions of high stress in human skeletal myofibers. Muscle Nerve 30, 337–346. [PubMed: 15318345]

Munoz-Marmol AM, Strasser G, Isamat M, Coulombe PA, Yang Y, Roca X, Vela E, Mate JL, Coll J, Fernandez-Figueras MT et al. (1998). A dysfunctional desmin mutation in a patient with severe generalized myopathy. Proc. Natl. Acad. Sci. USA 95, 11312–11317. [PubMed: 9736733]

O'Neill A, Williams MW, Resneck WG, Milner DJ, Capetanaki Y and Bloch RJ (2002). Sarcolemmal organization in skeletal muscle lacking desmin: evidence for cytokeratins associated with the membrane skeleton at costameres. Mol. Biol. Cell 13, 2347–2359. [PubMed: 12134074]

Pardo JV, Siliciano JD and Craig SW (1983). A vinculin-containing cortical lattice in skeletal muscle: transverse lattice elements ("costameres") mark sites of attachment between myofibrils and sarcolemma. Proc. Natl. Acad. Sci. USA 80, 1008–1012. [PubMed: 6405378]

Paulin D, Huet A, Khanamyrian L and Xue Z (2004). Desminopathies in muscle disease. J. Pathol 204, 418–427. [PubMed: 15495235]

Philippi M and Sillau AH (1994). Oxidative capacity distribution in skeletal muscle fibers of the rat. J. Exp. Biol 189, 1–11. [PubMed: 7964383]

Porter GA, Dmytrenko GM, Winkelmann JC and Bloch RJ (1992). Dystrophin colocalizes with β-spectrin in distinct subsarcolemmal domains in mammalian skeletal muscle. J. Cell Biol 117, 997–1005. [PubMed: 1577872]

Reed PW, Mathews KD, Mills KA and Bloch RJ (2004). The sarcolemma in the Large myd mouse. Muscle Nerve 30, 585–595. [PubMed: 15389724]

Reed P, Porter NC, Strong J, Pumplin DW, Corse AM, Luther PW, Flanigan KM and Bloch RJ (2006). Sarcolemmal reorganization in facioscapulohumeral muscular dystrophy. Ann. Neurol 59, 289–297. [PubMed: 16437580]

Reipert S, Steinbock F, Fischer I, Bittner RE, Zeold A and Wiche G (1999). Association of mitochondria with plectin and desmin intermediate filaments in striated muscle. Exp. Cell Res 252, 479–491. [PubMed: 10527638]

Renley BA, Rybakova IN, Amann KJ and Ervasti JM (1998). Dystrophin binding to nonmuscle actin. Cell Motil. Cytoskeleton 41, 264–270 [PubMed: 9829780]

Rybakova IN and Ervasti JM (2005). Identification of spectrin-like repeats required for high affinity utrophin-actin interaction. J. Biol. Chem 280, 23018–23023. [PubMed: 15826935]

Rybakova IN, Amann KJ and Ervasti JM (1996). A new model for the interaction of dystrophin with F-actin. J. Cell Biol 135, 661–672. [PubMed: 8909541]

Rybakova IN, Patel JR and Ervasti JM (2000). The dystrophin complex forms a mechanically strong link between the sarcolemma and costameric actin. J. Cell Biol 150, 1209–1214. [PubMed: 10974007]

Sam M, Shah S, Friden J, Milner DJ, Capetanaki Y and Lieber RL (2000). Desmin knockout muscles generate lower stress and are less vulnerable to injury compared wildtype muscles. Am. J. Physiol. Cell Physiol 279, C1116–C1122. [PubMed: 11003592]

Schroder R, Kunz WS, Rouan F, Pfendner E, Tolksdorf K, Kappes-Horn K, Altenschmidt-Mehring M, Knoblich R, van der Ven PF, Reimann J et al. (2002). Disorganization of the desmin cytoskeleton and mitochondrial dysfunction in plectin-related epidermolysis bullosa simplex with muscular dystrophy. J. Neuropathol. Exp. Neurol 61, 520–530. [PubMed: 12071635]

Schroder R, Goudeau B, Simon MC, Fischer D, Eggermann T, Clemen CS, Li Z, Reimann J, Xue Z, Rudnik-Schoneborn S et al. (2003). On noxious desmin: functional effects of a novel heterozygous desmin insertion mutation on the extrasarcomeric desmin cytoskeleton and mitochondria. Hum. Mol. Genet 12, 657–669. [PubMed: 12620971]

Senter L, Luise M, Presotto C, Betto R, Teresi A, Ceoldo S and Salviati G (1993). Interaction of dystrophin with cytoskeletal proteins: binding to talin and actin. Biochem. Biophys. Res. Commun 192, 899–904. [PubMed: 8484792]

Shah SB, Davis J, Weisleder N, Kostavassili I, McCulloch AD, Ralston E, Capetanaki Y and Lieber RL (2004). Structural and functional roles of desmin in mouse skeletal muscle during passive deformation. Biophys. J 86, 2993–3008. [PubMed: 15111414]

Sjoberg G, Saavedra-Matiz CA, Rosen DR, Wijsman EM, Borg K, Horowitz SH and Sejersen T (1999). A missense mutation in the desmin rod domain is associated with autosomal dominant distal myopathy, and exerts a dominant negative effect on filament formation. Hum. Mol. Genet 8, 2191–2198. [PubMed: 10545598]

Stone MR, O'Neill A, Catino D and Bloch RJ (2005). Specific interaction of the actin-binding domain of dystrophin with intermediate filaments containing keratin 19. Mol. Biol. Cell 16, 4280–4293. [PubMed: 16000376]

Sutherland-Smith AJ, Moores CA, Norwood FL, Hatch V, Craig R, Kendrick-Jones J and Lehman W (2003). An atomic model for actin binding by the CH domains and spectrin-repeat modules of utrophin and dystrophin. J. Mol. Biol 329, 15–33. [PubMed: 12742015]

Tamai Y, Ishikawa T, Bosl MR, Mori M, Nozaki M, Baribault H, Oshima RG and Taketo MM (2000). Cytokeratins 8 and 19 in the mouse placental development. J. Cell Biol 151, 563–572. [PubMed: 11062258]

Teixeira CFP, Zamuner SR, Zuliani JP, Fernandes CM, Cruz-Hofling MA, Fernandes I, Chaves F and Gutierrez JM (2003). Neutrophils do not contribute to local tissue damage, but play a key role in skeletal muscle regeneration, in mice injected with *Bothrops asper* snake venom. Muscle Nerve 28, 449–459. [PubMed: 14506717]

Toivola DM, Tao G-Z, Habtezion A, Liao J and Omary MB (2005). Cellular integrity plus: organelle-related and protein-targeting functions of intermediate filaments. Trends Cell Biol 15, 608–617. [PubMed: 16202602]

Ursitti JA, Martin L, Resneck WG, Chaney T, Zielke C, Alger BE and Bloch RJ (2001). Spectrins in developing rat hippocampal cells. Dev. Brain Res 129, 81–93. [PubMed: 11454415]

Ursitti JA, Lee PC, Resneck WG, McNally MM, Bowman AL, O'Neill A, Stone MR and Bloch RJ (2004). Cloning and characterization of cytokeratins 8 and 19 in adult rat striated muscle: interaction with the dystrophin glycoprotein complex. J. Biol. Chem 279, 41830–41838. [PubMed: 15247274]

Warner LE, DelloRusso C, Crawford RW, Rybakova IN, Patel JR, Ervasti JM and Chamberlain JS (2002). Expression of Dp260 in muscle tethers the actin cytoskeleton to the dystrophin-glycoprotein complex and partially prevents dystrophy. Hum. Mol. Genet 11, 1095–1105. [PubMed: 11978768]

Williams MW and Bloch RJ (1999). Extensive but coordinated reorganization of the membrane skeleton in myofibers of dystrophic (mdx) mice. J. Cell Biol 144, 1259–1270. [PubMed: 10087268]

Yan Z, Choi S, Liu X, Zhang M, Schageman JJ, Lee SY, Hart R, Lin L, Thurmond FA and Williams RS (2003). Highly coordinated gene regulation in mouse skeletal muscle regeneration. J. Biol. Chem 278, 8826–8836. [PubMed: 12477723]

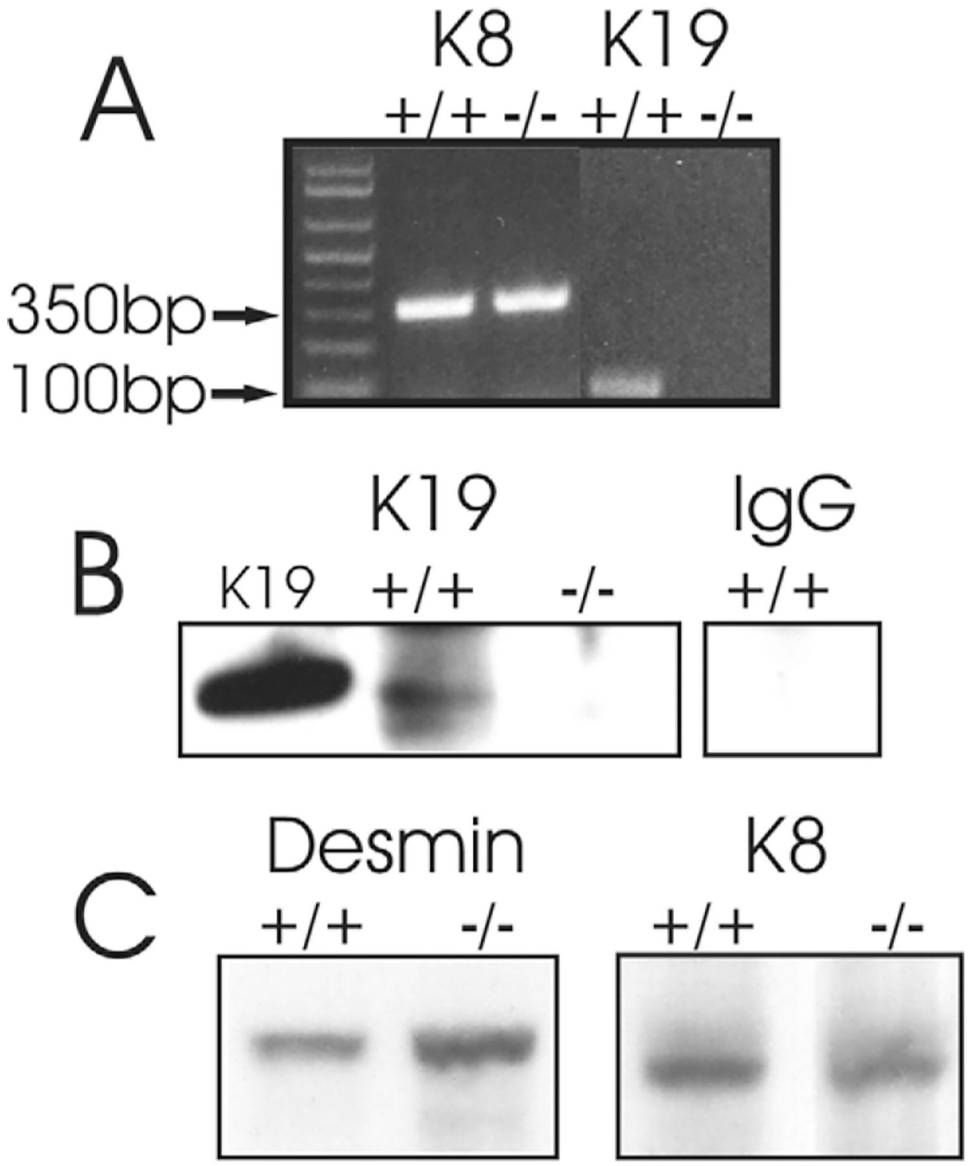

Fig. 1.

Analysis of mutant mice for the presence of K19. (A) Extracts of muscle were analyzed by RT-PCR for the presence of mRNA encoding K8 and K19. $K19^{-/-}$ extracts contained mRNA encoding K8, at levels similar to controls, but lacked mRNA encoding K19. (B) K19 was immunoprecipitated from extracts of TA muscle from wild-type or $K19^{-/-}$ mice, then immunoblotted with anti-K19 antibodies. Lanes show immunoblots of: K19, purified K19; +/+, immunoprecipitate from wild-type muscle; −/−, immunoprecipitate from $K19^{-/-}$ muscle; IgG, immunoprecipitate from wild-type muscle probed with a non-immune control (MOPC). Equal loading and transfer was confirmed by Ponceau S staining (not shown). K19 was not detected in muscle of $K19^{-/-}$ mice. (C) Immunoblots of desmin and K8 in extracts of TA muscle from wild-type (+/+) and $K19^{-/-}$ mice. Desmin is slightly but significantly elevated in the $K19^{-/-}$ TA muscle compared with wild type; K8 levels are unchanged.

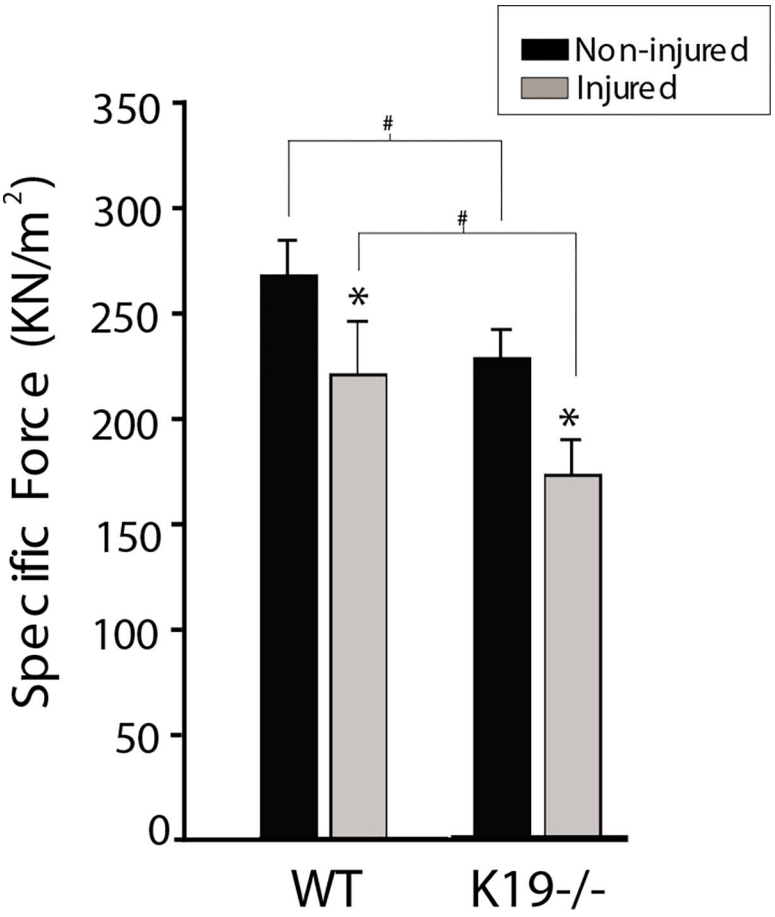

Fig. 2.

Measurement of specific force and susceptibility to eccentric injury. Maximal tetanic tension was measured in wild-type (WT) and K19$^{-/-}$ TA muscles before (black bars) and after (gray bars) injury caused by a single high-strain lengthening contraction. Data are reported as specific force (force normalized to cross-sectional area). Details are provided in Materials and Methods. Six animals were tested in each group. *$P \leqslant 0.001$, significant difference between non-injured and injured; $^{\#}P \leqslant 0.003$, significant difference between WT and K19$^{-/-}$. The differences in the extent of injury between WT and K19$^{-/-}$ were not significant (see text).

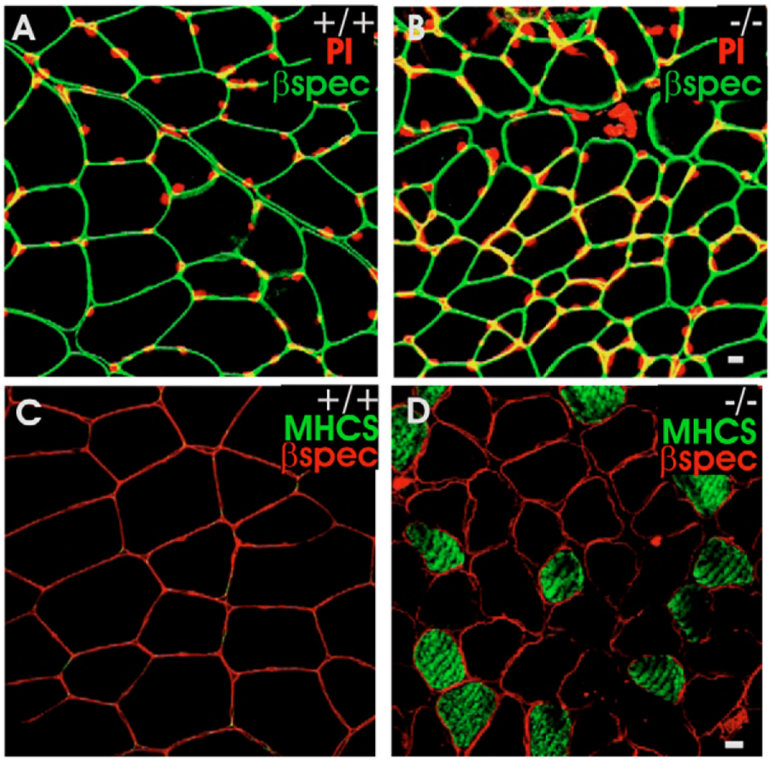

Fig. 3.

Fiber type, nuclear location and size of $K19^{-/-}$ myofibers. (A,B) TA muscles from wild-type (A) and $K19^{-/-}$ (B) mice were snap frozen, cryosectioned (20-μm cross sections) and fluorescently immunolabeled with antibodies against βI-spectrin to visualize the sarcolemma of the myofibers (shown in green), and counterstained with propidium iodide (PI) to visualize myonuclei (shown in red). Many fibers in $K19^{-/-}$ muscle were smaller than controls but did not have central nuclei. (C,D) Cross sections of mouse TA muscle were labeled with antibodies against βI-spectrin (red) and antibodies against the myosin heavy chain of slow-twitch muscle (MHCS; green). $K19^{-/-}$ muscle (D) showed ~10% of fibers labeled for the slow isoform of myosin, whereas wild-type muscle showed none (C). Bars, 5 μm.

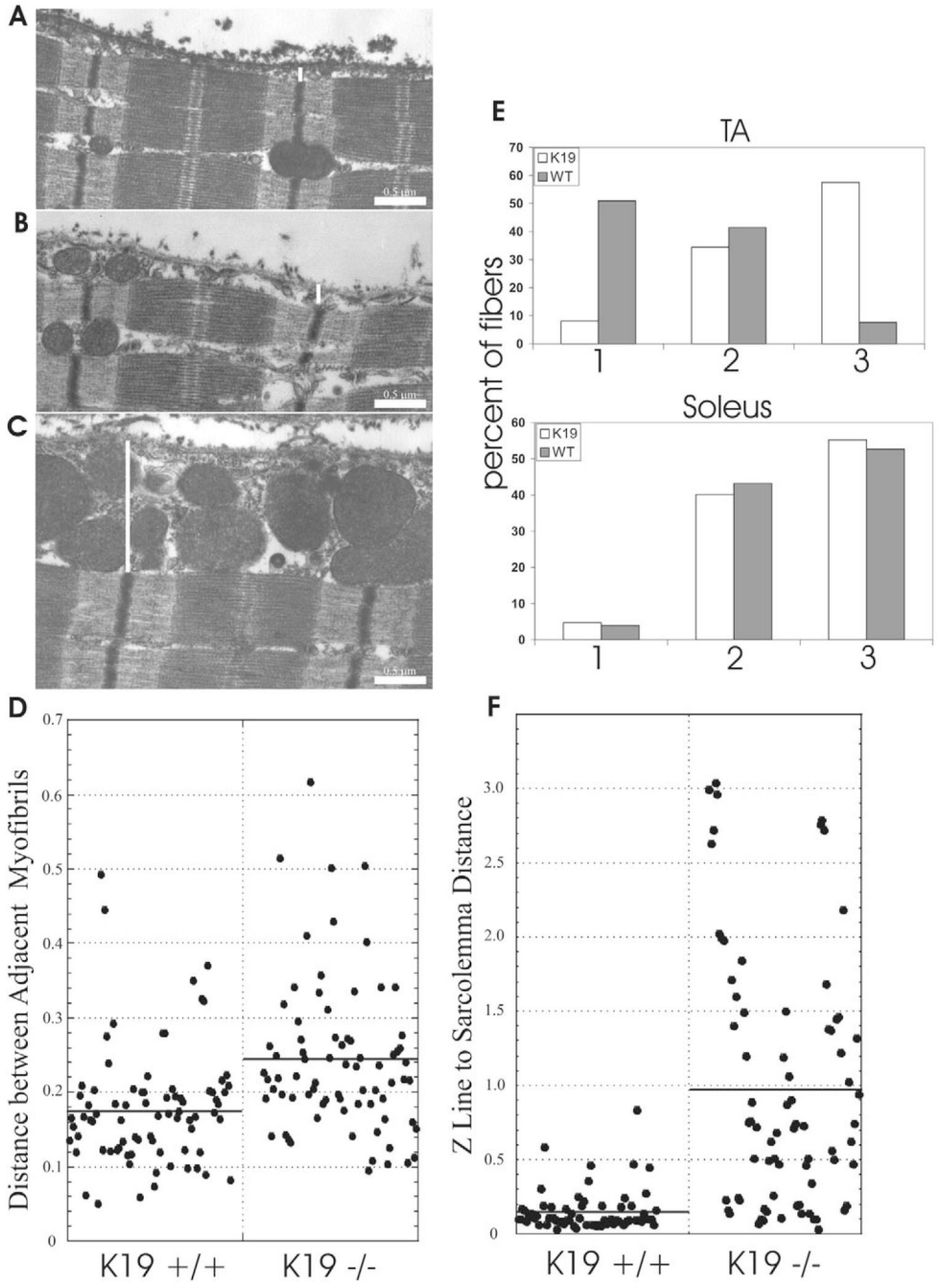

Fig. 4.

Ultrastructure of subsarcolemmal region of control and K19$^{-/-}$ muscle fibers. (A-C) TA muscles of control (A) and K19$^{-/-}$ (B,C) mice were fixed in situ, processed for electron microscopy of longitudinal thin sections, and viewed near the fiber surfaces. The distance between the sarcolemma and the nearest Z-disks (white lines) was greater in K19$^{-/-}$ samples (B,C) than in controls (A). Mitochondria accumulated in the subsarcolemmal gap to moderate (B) or large (C) extents in mutant but not in control (A) muscle. Sarcomeres in the mutant appeared unchanged. (D) Distances between neighboring Z-disks in adjacent

myofibrils were measured and are shown in μm. Control values were ~180 nm (line). $K19^{-/-}$ samples showed a mean value of ~240 nm (line). These differences are highly significant (see text). (E) The percent myofibers with slight (category 1), moderate (category 2) or large (category 3) accumulations of mitochondria under the sarcolemma (see Materials and Methods) were scored in TA and soleus muscle fibers of wild-type (gray bars) and $K19^{-/-}$ (white bars) mice. TA but not soleus muscle showed significant increases in the number of myofibers with large numbers of subsarcolemmal mitochondria. (F) Distances between the sarcolemma and the nearest Z-disks were measured and are shown in μm. Control values were ~150 nm, with little variation (line). $K19^{-/-}$ samples showed a mean value of ~1 μm, with greater variation (line). These differences are highly significant (see text).

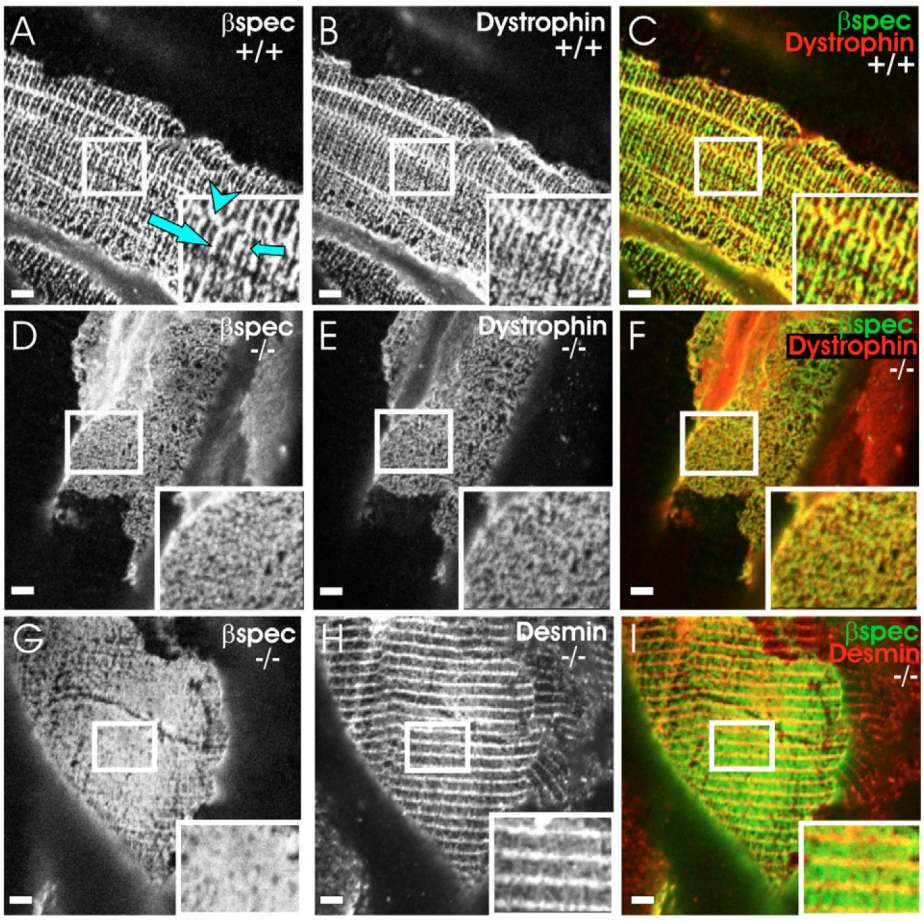

Fig. 5.

Costameres at the sarcolemma of K19$^{-/-}$ muscle are disrupted. Frozen, longitudinal cryosections of tibialis anterior muscles from wild-type (A-C) and K19$^{-/-}$ (D-I) mice were immunofluorescently labeled with pairs of antibodies to membrane skeletal proteins at the sarcolemma (βI-spectrin: A,D,G; dystrophin: B,E) and nearby structures (desmin, H). Color overlays (C,F,I) show βI-spectrin in red (C,F) or green (I), and the other proteins in the contrasting color. Regions labeled by both antibodies are shown in yellow. Insets show twofold magnifications of the boxed areas in each panel. The results show that the normally rectilinear pattern of costameres (A-C; large arrow indicates a Z-domain; small arrow indicates an M-domain; arrowhead indicates an L-domain) is disrupted in K19$^{-/-}$ muscle (these domains are missing in the examples shown in D-I) without, however, altering the organization of desmin in nearby myofibrils (H,I). Bars, 5 μm.

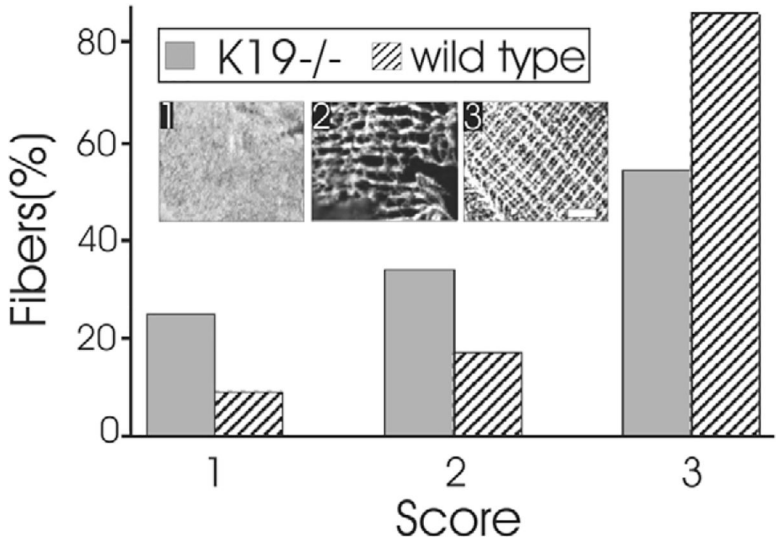

Fig. 6.

Quantitation of costameric organization in K19$^{-/-}$ myofibers. Longitudinal sections tangential to the sarcolemma of myofibers were labeled with antibodies against βI-spectrin, and costameres were scored as extensively disrupted (category 1, panel 1; see also Fig. 5D,G), moderately disrupted, with only one set of costameric domains remaining (category 2, panel 2), or normal, with costameres present over Z- and M-lines and oriented longitudinally as well (category 3, panel 3; see also Fig. 5A). Costameres in the K19$^{-/-}$ fibers (gray bars) were significantly more disrupted than in controls (striped bars; see text).

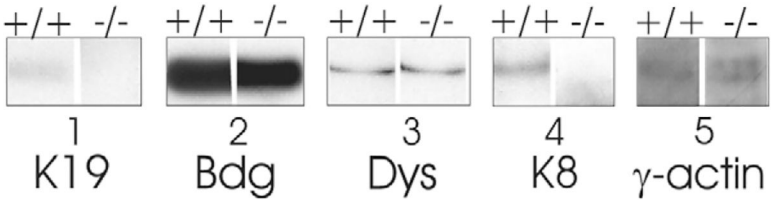

Fig. 7.

Isolation of the dystrophin-dystroglycan complex of the $K19^{-/-}$ mouse. The dystrophin-dystroglycan complex was partially purified on a wheat germ lectin affinity column, eluted, and analyzed by SDS-PAGE and immunoblotting, as described in Materials and Methods. K19, K8 and γ-actin eluted with dystrophin (Dys) and β-dystroglycan (Bdg) from control tissue, but only γ-actin eluted with these proteins from $K19^{-/-}$ tissue.

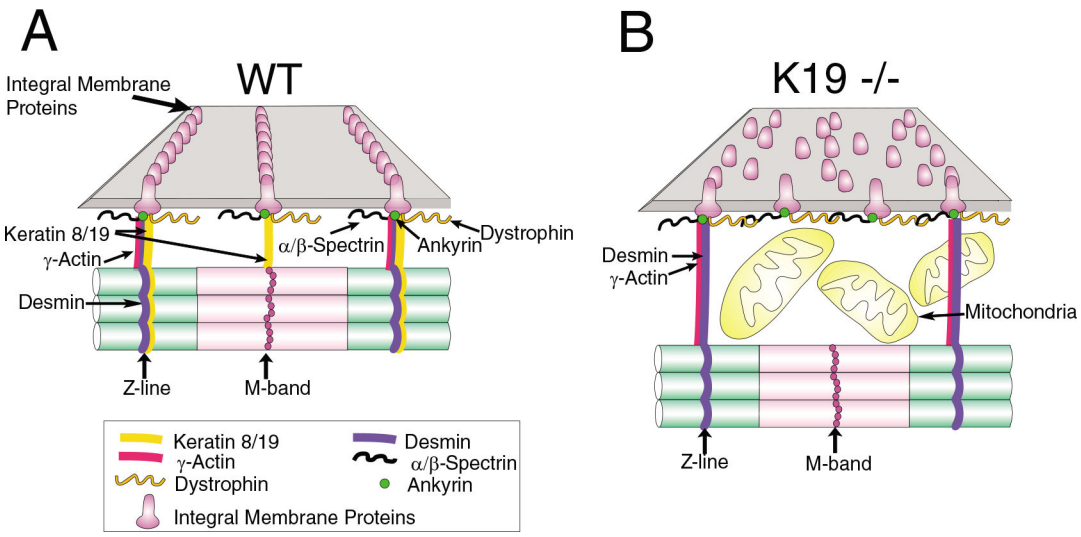

Fig. 8.

Effect of $K19^{-/-}$ mutation on costameres and nearby structures. (A) Organization of the costameres in the myofibrils of striated muscle. Image is adapted from Ursitti et al. (Ursitti et al., 2004). For clarity, only the Z- and M-domains of costameres and a few of the integral and peripheral proteins present at costameres are shown. Emphasis is on the alignment of integral and peripheral membrane proteins with filaments composed of γ-actin, desmin, and K8 and K19. (B) Changes documented by us in $K19^{-/-}$ TA muscle, including the disruption of costameres, and the increase in the gap between the sarcolemma and the nearest myofibrils in which mitochondria accumulate. The retention of costameres in some $K19^{-/-}$ myofibers might be owing to filaments composed of γ-actin and desmin that persist in the absence of K19. Not drawn to scale.

Table 1.

Properties of normal and $K19^{-/-}$ TA muscles

	Control	$K19^{-/-}$
Minimal Feret's diameter	13.9±3.1	11.3±3.4 *
Muscle mass (mg)	31±1.5	28.2±2.7
Twitch tension (mN)	352±137	205±58
Tetanic tension (mN)	1122±22	940±47 *
Fatigue index (%)	80±12	79±14
Resting length (mm)	11.7±1.0	10.8±1.0
Evans-Blue-dye-labeled (%)	0	0
Central nuclei (%)	2	4
Plasma creatine kinase (U/l)	70±22	234±29 **
MHC-slow labeled (%)	0	10±6 **

All data are presented as the mean±s.d. Fatigue index (in %) is the maximal tetanic tension (P_0) after stimulation for 5 minutes at 1 Hz. Six animals in each group were assayed for mass, twitch and tetanic tension, fatigue and resting length. Three animals in each group were diameter, labeling was done using Evans Blue dye, central nuclei, plasma creatine kinase, and labeling for slow-twitch myofibers. MHC-slow, the percent myofibers labeled for the slow-twitch isoform of the myosin heavy chain.

* $P<0.001$ and

** $P<0.05$, statistically significant differences between $K19^{-/-}$ and control.